Revisiting atomic force microscopy force spectroscopy sensitivity for single molecule studies

Shahid Naeem,[1] Yu Liu,[1] Heng-Yong Nie,[2] W. M. Lau,[2] and Jun Yang[1,a)]

[1]*Department of Mechanical and Materials Engineering, University of Western Ontario, London, Ontario, N6A 5B9, Canada*
[2]*Surface Science Western, University of Western Ontario, London, Ontario, N6A 5B7, Canada*

Recently, the rapid advances in quantitative biology and polymer science have led to the atomic force microscope (AFM) being extensively employed for single-molecule force spectroscopy. Deflection sensitivity, a critical factor in single molecule force spectroscopy, is changed due to the change in bending shape of AFM cantilever when a single molecule is attached to the AFM cantilever tip. We quantitatively study this variation in the deflection sensitivity by modeling the single molecule as an AFM tip coupled spring. We further propose correction factors for the deflection sensitivity in various cases of single molecule studies. Since many single biomolecule studies are conducted in aqueous environment, we outline and include the complications induced by the refractive index discontinuity at the air-glass-liquid medium interfaces, laser spot size, and spot location on the cantilever. Finally we present correction factor charts for easy calculation of correction factors for a wide variety of stiffness of single molecules. © *2008 American Institute of Physics*. [DOI: 10.1063/1.3037206]

I. INTRODUCTION

In recent years, there has been an explosion in the use of atomic force microscopy (AFM) for single molecule studies.[1–4] These studies have realized measurements of molecular forces at the piconewton level for DNA base pairings,[5] ligand-receptor pairs,[6] protein intramolecular structural interactions,[7] and strength of covalent bonds.[8] The fundamental principle is the coupling of an AFM cantilever probe tip to a molecule of interest, controlling movement of the piezoelectric AFM Z-scanner and simultaneously monitoring stretch/compress force via the laser reflection onto a photosensitive diode.

The force exerted on a molecule by the probe tip at the free end of the cantilever is measured by the deflection of the cantilever multiplied by its spring constant.[9] The precision and accuracy of the force measurements depend critically on the ability to detect deflection of the AFM cantilever and accurate calibration of the spring constant. For an optical detection scheme AFM, a laser spot irradiated on the cantilever is used to detect the deflection of the cantilever with a photodetector. The detected cantilever deflection signal is the output of the photodetector. It is thus necessary to calibrate this photodetector signal to the deflection of the cantilever. This is done by moving the cantilever a known distance against a hard surface and measuring the photodetector output. The ratio of the known cantilever movement distance to the photodetector signal output is the deflection sensitivity (units, nm/V) of the optical detecting system also called inverse optical lever sensitivity (InVOLS).[10]

The thermal noise approach for spring constant estimation has appeared to be the most practical way to estimate the spring constant. The spring constant is calculated by collecting noise of the optical detector signal due to thermal fluctuation of the cantilever with time and using Fourier transformation to obtain the power density spectrum. The power in the first cantilever resonant mode is then multiplied with the deflection sensitivity and input into the equipartition theorem to obtain the cantilever spring constant. The accuracy of the method has been accepted in the force microscopy community.[10] Thus, accurate deflection sensitivity must be obtained in order to measure the force accurately. However, the photodetector is sensitive to the cantilever bending shape rather than to the cantilever deflection.[11] The bending shape varies depending on whether the cantilever is deflected by a localized static force at the end, or it is vibrating freely driven by thermal fluctuation, or if it is vibrating with a coupled single molecule.[12–14] Hence, the deflection sensitivity is changed from case to case according to the variance of bending shape and may need to be corrected.

We employ a general coupled spring model[14] to study the deflection sensitivity and finally provide quantitative values for the correction factor when a single molecule is linked between the AFM tip and the substrate, as illustrated in the Fig. 1. Furthermore most single molecule experiments, especially biological ones, are conducted under aqueous environment. It has been recognized that deflection sensitivity changes when AFM is operated under aqueous condition.[15,16] This is primarily due to the refractive index discontinuities, which couples with the changes in laser spot size and spot location on the cantilever.[17] We include the considerations for aqueous environment in our study as well to quantify the coupled effects on deflection sensitivity for accurate force measurements.

a)Author to whom correspondence should be addressed. Tel.: (519) 661 2111 ext. 80158. FAX: (519) 6613020. Electronic mail: jyang@eng.uwo.ca.
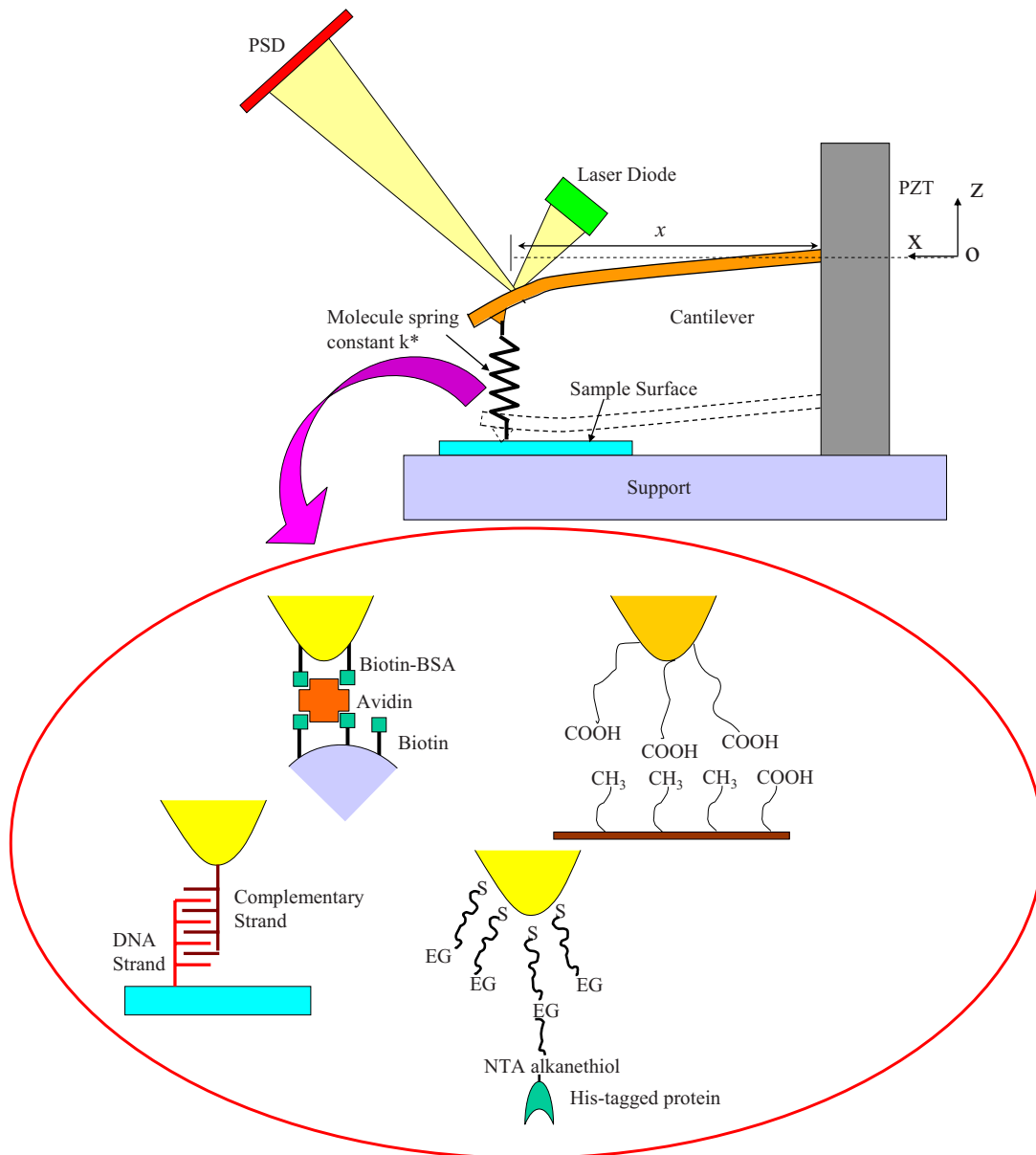
FIG. 1. (Color online) Single molecule experimental setup and the spring coupled model. The inset shows different single molecules setups. [Force induced DNA slippage (Ref. 27), receptor ligand (Ref. 28), recombinant histidine-tagged proteins attached onto an AFM tip coated with NTA-terminated alkanethiols (Ref. 29) and adhesive forces between CH_3−COOH groups (Ref. 30)].

II. THEORY

A. Flexible beam model

The AFM cantilever beam can be ideally modeled as a flexible beam with homogeneous uniform cross section.[10,14] For a flexible cantilever, with one end clamped at its base and the other end static force loaded, the normalized shape function $h(x)$ is given by[9,18]

$$h_{end}(x) = \frac{3x^2 - x^3}{2},$$ (1)

where x is the laser spot location calculated from the base of the cantilever.

For evaluating the shape functions of a freely vibrating or spring coupled cantilever at its first vibration mode, simi-

lar methodology has been employed for both cases by Rabe *et al.*[14] Considering a flexible uniform cross section homogenous beam for its flexural vibrations, the equation of motion can be expressed by the fourth-order ordinary differential equation

$$EI\frac{\partial^4 z}{\partial x^4} + \rho A\frac{\partial^2 z}{\partial t^2} = 0,$$ (2)

where E is the Young's modulus, ρ is the mass density, A is the cross section area, and I is the area moment of inertia. x is the coordinate in the longitudinal direction of the cantilever, as shown in Fig. 1. $z(x)$ is the deflection from the rest position of the length element at x location of the cantilever. A general solution to the Eq. (2) of motion is

$$h(x) = A'(\cos k_n x + \cosh k_n x) + B'(\cos k_n x - \cosh k_n x)$$
$$+ C'(\sin k_n x + \sinh k_n x) + D'(\sin k_n x - \sinh k_n x), \quad (3)$$

where k_n is the wave number of the beam at its first flexural vibration mode ($n=1$) and A', B', C', and D' are the constants to be determined using boundary conditions. For a cantilever with one end clamped and the other end spring coupled as shown in Fig. 1, a deflection z adds to the shear force $(-k^*z)$,[14]

$$EI\frac{\partial^3 z}{\partial x^3} - k^* z = 0, \quad (4)$$

where k^* is the stiffness of the attached spring. Using the following boundary conditions:[14]

$$h(x) = 0, \frac{\partial h(x)}{\partial x} = 0 \quad \text{at} \ x = 0,$$

$$\frac{\partial^2 h(x)}{\partial x^2} = 0, \frac{\partial^3 h(x)}{\partial x^3} = \frac{3k^*}{k_c L^3} h(x) \quad \text{at} \ x = 0, \quad (5)$$

we obtain the characteristic equation

$$\sinh k_n L \cos k_n L - \sin k_n L \cosh k_n L$$
$$= \frac{(k_n L)^3 k_c}{3k^*}(1 + \cos k_n L \cosh k_n L), \quad (6)$$

where k_c is the cantilever stiffness and L is the length of the cantilever. When $k^*=0$, Eq. (6) becomes that of a freely vibrating cantilever. Based on aforementioned boundary conditions, we simplify the Eq. (3) to

$$h_{\text{spring}}(x) = G(\cos k_n x - \cosh k_n x) + H(\sin k_n x - \sinh k_n x), \quad (7)$$

where G and H are coefficients of the shape function $h(x)$.[10,12] The one-dimensional irradiance distribution of a Gaussian laser beam (generally assumed) along the cantilever x-axis has been given in literature[12,19]

$$I(x) = \sqrt{\frac{8}{\pi}}\frac{P_0}{w_0}\exp\left(\frac{-8(x-x_c)^2}{(w_0)^2}\right), \quad (8)$$

where P_0 is the total power from the laser diode and w_0 is the focused optical spot size in the plane perpendicular to the axis of the incident beam at the $1/e$ irradiation points. $x_c = \gamma L_{\text{eff}}$ is the center location of Gaussian spot along x-axis with γ standing for the relative location on the cantilever ($0 < \gamma < 1.0$)[10,17] and L_{eff} is the effective cantilever length equal to $L \cos \theta_{\text{tilt}}$.[12] θ_{tilt} is the angle of the cantilever with the horizontal. Correspondingly, the scalar wave function of a Gaussian incident beam is[18]

$$E(x) = \sqrt{\sqrt{\frac{8}{\pi}}\frac{P_0}{w_0}}\exp\left(\frac{-4(x-x_c)^2}{(w_0)^2}\right). \quad (9)$$

The photodetector deflection signal output of optic lever detection AFM system caused by the phase shift in waves of a coherent laser along the cantilever axis due to the "functional shape" of a cantilever is[12]

$$D(z) = \frac{4z\alpha}{\lambda}\int_0^{L_{\text{eff}}} dx \int_0^{L_{\text{eff}}} dx' E(x)E(x')$$
$$\times \frac{h(x/L_{\text{eff}}) - h(x'/L_{\text{eff}})}{x - x'}, \quad (10)$$

where α is the loss factor of the laser power incident on photodetector, λ is the wavelength of detection laser light (assumed here $\lambda = 810$ mm), and z is the cantilever deflection in the z-direction. In our analysis, we assume that there is no power loss for laser transmitting in the space and α is equal to one. $h(x/L_{\text{eff}})$ is the normalized shape function equation chosen according to the cantilever loading conditions.

B. Model for spring coupled cantilever in liquid

When AFM is employed in liquid, the focal length of the focus lens is extended due to discontinuity of refractive index at air-glass interface and glass-liquid interface.[17] Our previous work[17] has used the following equation to solve the shifted displacement ΔL_1 due to increased focal length:

$$\Delta L_1 = h_2 \frac{n_{\text{liq}} - n_{\text{glass}}}{n_{\text{glass}}} + \Delta L_2 \frac{n_{\text{liq}}}{n_{\text{glass}}}, \quad (11)$$

where h_2 is the layer thickness of the liquid, n_{liq} and n_{glass} are the refractive indexes of liquid and glass, respectively. ΔL_2 is the shifting of laser beam in liquid when the refractive index of the liquid is the same as that of glass and is expressed by the relationship

$$\Delta L_2 = (h_1 + h_2)\frac{n_{\text{glass}} - n_{\text{air}}}{n_{\text{air}}}, \quad (12)$$

where h_1 is the layer thickness of the glass plane and n_{air} is the refractive index of air. Hence, the extension of the focal length ΔL_1 in liquid is dependent on the discontinuity of the refractive indices, coupled with the layer thickness of glass h_1 and liquid h_2.

This extended focal length directly changes the spot size on the back face of the cantilever. This changed spot size can be calculated by[20–22]

$$w' = w_0\left\{1 + \left(\frac{4\lambda\Delta L_1}{\pi w_0^2 n_{\text{liq}}}\right)^2\right\}^{1/2}, \quad (13)$$

where w_0 and w' are the spot sizes along x-axis at irradiance points in air and in liquid, respectively. The spot size on the cantilever plane is increased on passing through liquid and glass.[17,23]

Under the liquid environment, the refractive index discontinuities at the air-glass and glass-liquid interfaces cause distortion in the beam path. To correct this distortion, we use the relationship between z, the deflection in air detected by photodetector, and z_{eff} the effective deflection detected by photodetector due to the refraction in the liquid environment,[17,24]

TABLE I. Numerical solutions of the Eq. (6) for the coefficient values of Eq. (7).

k^*/k_c	$k_n L$	G	H
0	1.8751	−0.5000	0.3670
0.05	1.8974	−0.4920	0.3612
0.1	1.9189	−0.4847	0.356
0.25	1.9790	−0.4660	0.3432
0.5	2.0675	−0.4428	0.3287
0.75	2.1448	−0.4265	0.3196
1	2.2135	−0.4147	0.3141

$$z_{\text{eff}} = \frac{\cos 2\theta_{\text{tilt}}}{\sqrt{\left(\frac{n_{\text{air}}}{n_{\text{liq}}}\right)^2 - \sin^2 2\theta_{\text{tilt}}}} z. \qquad (14)$$

The photodetector deflection signal equation $D(z)$ Eq. (10) for liquid can therefore be written as

$$D_{\text{liq}}(z) = z_{\text{eff}} \frac{4\alpha}{\lambda} \int_0^{L_{\text{eff}}} dx \int_0^{L_{\text{eff}}} dx' E(x) E(x')$$

$$\times \frac{h(x/L_{\text{eff}}) - h(x'/L_{\text{eff}})}{x - x'}. \qquad (15)$$

Here $E(x)$ the scalar laser wave function from Eq. (9) would be calculated using w' instead of w_0.

In this study, we quantitatively investigate the modified deflection sensitivity correction factor $\chi = \text{InvOLS}_{\text{spring}}/\text{InvOLS}_{\text{end}} = D_{\text{end}}(z)/D_{\text{spring}}(z)$, originally proposed by Proksch *et al.*,[10] for various values of spring stiffness to cantilever stiffness ratio (k^*/k_c), and for both air and liquid cases.

III. RESULTS AND DISCUSSION

Using the characteristic Eq. (6) for spring coupled cantilevers, we get the values for the fundamental vibration mode of the cantilever, listed in Table I.

A. Correction factor χ in air

Using the values in Table I for the normalized shape function Eq. (7), the normalized deflection of the cantilever along its length is shown in Fig. 2 for various k^*/k_c ratios. The static end loaded cantilever deflection, given by Eq. (1), is also shown.

The photodetector deflection sensitivity is dependent more on the cantilever bending slope the laser is reflecting off, rather than the deflection of the cantilever.[11] The cantilever slope varies along the cantilever length as well as with different end loads. The deflection variance along the cantilever length in Fig. 2 for various coupled spring stiffness shows this bending slope variance. To make this point clearer, Fig. 3 shows the first derivative (slope) of the shape function equations of the cantilevers with various coupled spring stiffness plotted along the length of the cantilever. The shape function derivative of the static end loaded cantilever is also shown in Fig. 3.
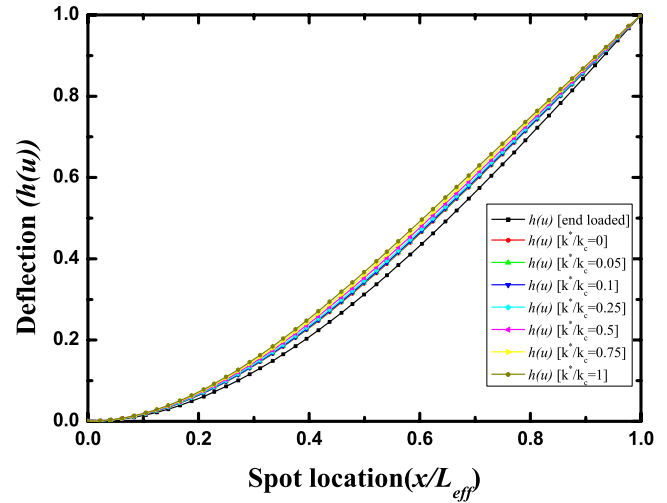

FIG. 2. (Color online) Deflection for various cantilever functional shapes.

The slope of the end loaded cantilever at its very end is 1.09 times that of the freely vibrating cantilever, as discussed in Refs. 11, 18, and 25, and has been assumed as the correction factor for freely vibrating cantilevers [$\chi = 1.09$ (Ref. 25)]. It can be seen in Fig. 3 that for the case of spring coupled cantilevers, the cantilever end slope difference is further enlarged, going up to $\chi = 1.20$ for the case of a coupled spring stiffness equal to cantilever stiffness $(k^* = k_c)$. These values for χ are only valid for the case of an infinitely small spot positioned at the very end of the cantilever beam.

Finite sized laser spot correction factor $\chi = \text{InvOLS}_{\text{spring}}/\text{InvOLS}_{\text{end}} = D_{\text{end}}(z)/D_{\text{spring}}(z)$ values plotted along the cantilever length for various values of k^*/k_c in air are shown in Fig. 4. For these calculations, we assume the spot size in air $w_0 = 51$ μm and the cantilever tilt $\theta_{\text{tilt}} = 10°$. Figure 4 quantitatively shows correction factors, relating the deflection sensitivity of spring coupled cantilever beam to that of end loaded cantilever, plotted along the cantilever length. The curve for the freely vibrating cantilever $(k^*/k_c = 0)$ gives $\chi(0) = 0.871$ at the base to $\chi(L_{\text{eff}}) = 1.083$ at the end, as found by Proksch *et al.*[10] For increasing values of
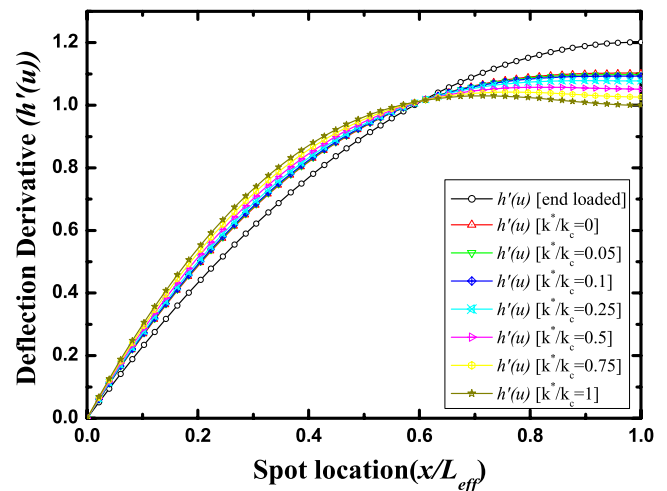

FIG. 3. (Color online) First derivatives of deflection (slope) for various cantilever shape functions.
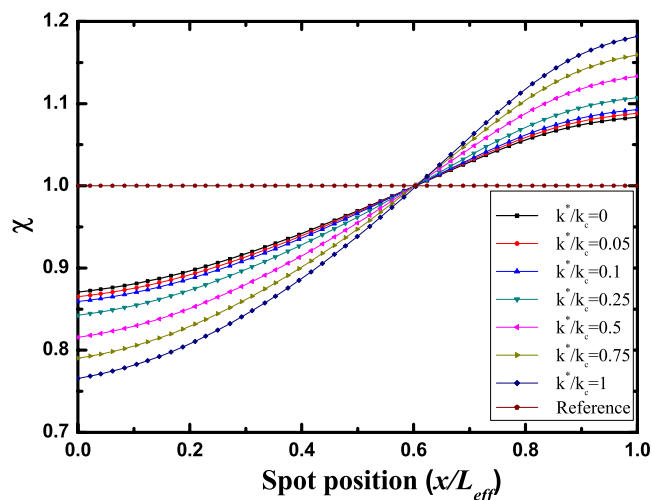
FIG. 4. (Color online) Correction factor ($\chi=D_{end}/D_{spring}$) in air for various cantilever functional shapes.

FIG. 5. Effect of liquid refractive index on spot size. Assumptions $w_0/2$ $=10$ μm, $h_1=1$ mm, $h_2=1.5$ mm, $n_{liq}=1.3$, $n_{glass}=1.55$, and $\lambda=810$ nm.

k^*/k_c, the curves show upward trends at the coupled end and downward trends at the base. For example, when $k^*/k_c=1$ the plot gives $\chi(0)=0.766$ at the base and $\chi(L_{eff})=1.182$ at the end. This is about 9%–13% difference in χ between $k^*/k_c=0$ and $k^*/k_c=1$ depending on the spot location along the cantilever.

Figure 4 also reveals the interesting result, for a normalized spot location (x/L_{eff}) around 0.6 the correction factor χ becomes 1 for all the different values of k^*/k_c. The reason for this phenomenon can be seen in Fig. 3, which shows all the deflection derivatives (slopes) to be the same around the 0.6 normalized spot location (x/L_{eff}). We have already mentioned that the photodetector output is sensitive to the cantilever slope rather than its deflection. As Fig. 3 shows, the slopes for all the cantilevers are equal around the 0.6 normalized spot location (x/L_{eff}) so the correction factor χ becomes 1. This implies the sensitivity to be same for the different cantilever end loadings at 0.6 normalized spot location (x/L_{eff}). In other words, when the spot is located at x/L_{eff} $=0.6$, the general sensitivity obtained by force-distance curve can be used directly in real-time single molecule studies to calculate the molecular force, or in thermal noise methods to calibrate the spring constant of cantilevers.[10] Otherwise, the real sensitivity during measurement should be multiplied by $1/\chi$. From Fig. 4, dependence of the sensitivity on the spot location suggests that we better locate the laser spot at $x/L_{eff}=0.6$. In literature,[26–30] a softer cantilever is always preferred in single molecule studies, which has a more sensitive response to small intermolecular force that is typically at the scale of piconewton. As shown in Fig. 4, if the cantilever is coupled with a single molecule spring, the real sensitivity due to free vibrating is degraded by about 10% when k_c is reduced from $10k^*$ to k^*. However if the laser spot is located at $x/L_{eff}=0.6$, there is no such worry.

B. Correction factor χ in liquid

Examining the effect of aqueous environment on the deflection sensitivity, Fig. 5 shows the relationship of spot size in liquid with the refractive index of the liquid (n_{liq}) as given

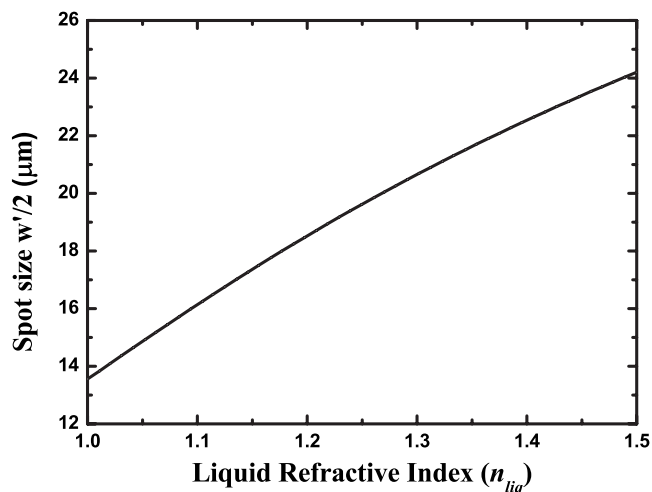by Eq. (13). Figure 5 illustrates the spot size increase in liquid with increasing liquid refractive index (n_{liq}), which is due to the coupled relationship between increased focal length and the refractive index of the liquid. The liquid medium has a magnifying effect on the laser spot size.

In general, the deflection sensitivity has to be recalibrated whenever a new cantilever is installed as the laser spot position on the cantilever is changed. The changed laser spot position samples a different cantilever slope, and hence affects the deflection sensitivity.[10]

In liquid, the deflection sensitivity is further affected due to the distortion produced by the different refractive media and the increased spot size. Hence, for applying the deflection sensitivity correction factors χ in liquid situation, it is necessary to use the end loaded deflection sensitivity in the liquid medium as reference. The χ factor values for liquid environment are shown in Fig. 6 where the end loaded cantilever photodetector deflection $[D_{end}(z)]$ in liquid is employed as reference. Figure 6 shows the correction factors χ in liquid, for the aforementioned assumptions made for the χ in air, with additional assumptions of the $n_{liq}=1.3$, n_{glass}
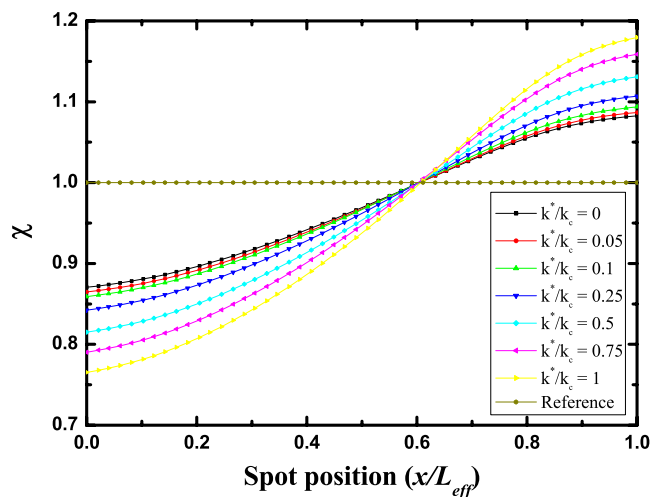

FIG. 6. (Color online) Correction factor ($\chi=D_{end}/D_{spring}$) in liquid for various cantilever functional shapes.
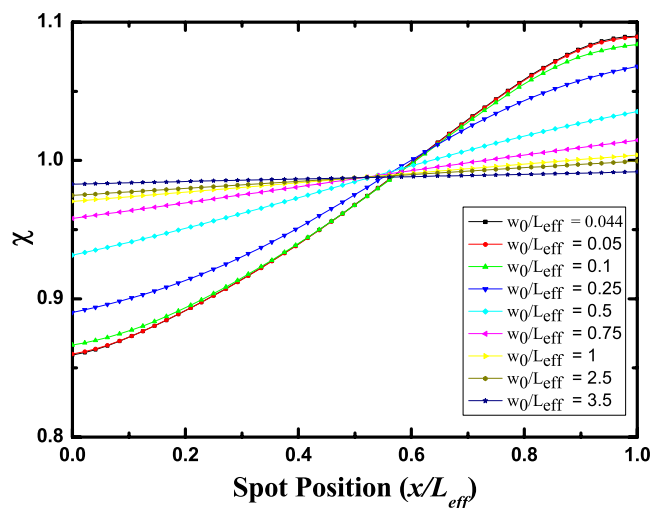
FIG. 7. (Color online) Correction factor ($\chi = D_{end}/D_{spring}$) in liquid for $k^*/k_c = 0$ for various w_0/L_{eff} ratios.

=1.55, and n_{air}=1. The thickness of the glass (h_1) and liquid medium (h_2) have been assumed to be 1 and 1.5 mm, respectively.[17]

It should be noted that the change in deflection sensitivity for various k^*/k_c ratios would be more significant for smaller spot sizes in air as we demonstrate in Figs. 7–9. This is because smaller spot sizes are magnified a lot more in liquid, as given by the relationship in Eq. (13). Figure 6 also shows the familiar χ=1 around normalized spot location of 0.6 along the cantilever length. Figures 8 and 9 show the correction factors in liquid for various ratios of spot diameter in air to effective cantilever length (w_0/L_{eff}), for k^*/k_c of 0.05 and 0.1, respectively. For reference, the freely vibrating case (k^*/k_c=0) is also presented in Fig. 7.

Since the AFM cantilever is generally considered very stiff for single molecule studies.[26] Therefore, we gave the correction factors χ for k^*/k_c=0.05 and 0.1, as these are expected to fall in the practical range of spring stiffness of single biomolecules. Figures 7–9 allow for the correction factor values to be read off the chart provided the laser spot
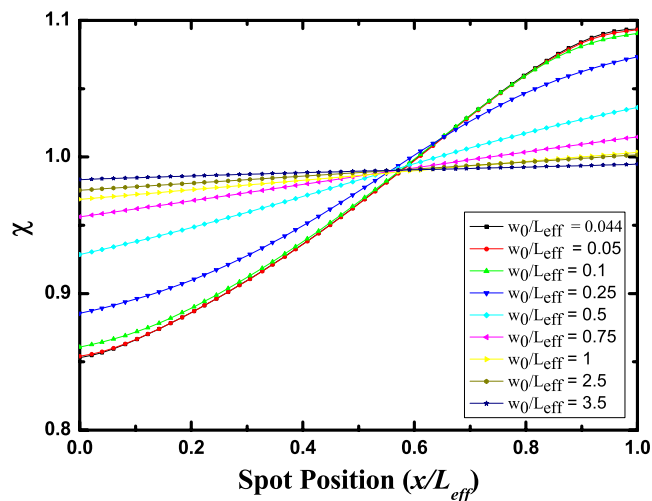

FIG. 8. (Color online) Correction factor ($\chi = D_{end}/D_{spring}$) in liquid for $k^*/k_c = 0.05$ for various w_0/L_{eff} ratios.
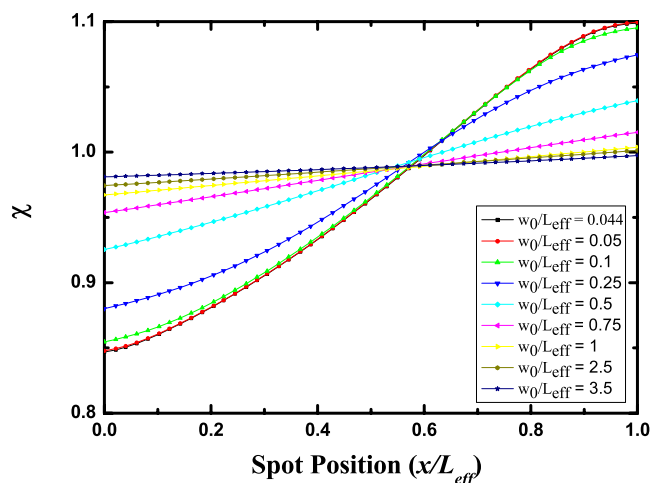

FIG. 9. (Color online) Correction factor ($\chi = D_{end}/D_{spring}$) in liquid for $k^*/k_c = 0.1$ for various w_0/L_{eff} ratios.

size in air, cantilever length, and spot location on the cantilever are known. These figures are especially useful due to the wide variety of cantilever sizes being used in single molecule studies. Smaller cantilevers have been suggested for both of image and force measurements due to advantages of lower noise levels and reduced hydrodynamic drags.[10,13,25] The finite spot size becomes even more significant for these cantilever lengths and the correction factor charts given here allow for accurate correction factor determination.

IV. CONCLUSION

Calibration of the deflection sensitivity is the key of AFM single molecule force spectroscopy, which is essential for accurate, repeatable, and quantitative force calculations. In this work, we have comprehensively covered the various theoretical parameters involved in the calibration of deflection sensitivity. We have shown the variation in deflection sensitivity of spring coupled cantilevers from that of the static end loaded and freely vibrating cantilevers. Correction factors for single molecule studies in air as well as liquid media have been tabulated for easy use. These correction factor values should be used in the single molecule force spectroscopy in order to avoid the large errors, which can result from the incorrect calculation of the deflection sensitivity.

[1]D. J. Muller and Y. F. Dufrene, Nat. Nanotechnol. **3**, 261 (2008).
[2]P. E. Marszalek, H. Lu, H. Li, M. Carrion-Vazquez, A. F. Oberhauser, K. Schulten, and J. M. Fernandez, Nature (London) **402**, 100 (1999).
[3]T. E. Fisher, P. E. Marszalek, and J. M. Fernandez, Nat. Struct. Biol. **7**, 719 (2000).
[4]H. Clausen-Schaumann, M. Seitz, R. Krautbauer, and H. E. Gaub, Curr. Opin. Chem. Biol. **4**, 524 (2000).

[5]M. Rief, H. Clausen-Schaumann, and H. E. Gaub, Nat. Struct. Biol. **6**, 346 (1999).

[6]J. Zlatanova, S. M. Lindsay, and S. H. Leuba, Prog. Biophys. Mol. Biol. **74**, 37 (2000).

[7]A. Janshoff, M. Neitzert, Y. Oberdörfer, and H. Fuchs, Angew. Chem., Int. Ed. **39**, 3213 (2000).

[8]M. Grandbois, M. Beyer, M. Rief, H. Clausen-Schaumann, and H. E. Gaub, Science **283**, 1727 (1999).

[9]D. Sarid, *Scanning Force Microscopy: With Applications to Electric, Magnetic, and Atomic Forces*, 2nd ed. (Oxford University Press, New York, 1994).

[10]R. Proksch, T. E. Schaffer, J. P. Cleveland, R. C. Callahan, and M. B. Viani, Nanotechnology **15**, 1344 (2004).

[11]H. J. Butt and M. Jaschke, Nanotechnology **6**, 1 (1995).

[12]T. E. Schaffer and P. K. Hansma, J. Appl. Phys. **84**, 4661 (1998).

[13]T. E. Schaffer, J. Appl. Phys. **91**, 4739 (2002).

[14]U. Rabe, K. Janser, and W. Arnold, Rev. Sci. Instrum. **67**, 3281 (1996).

[15]G. Haugstad and W. L. Gladfelter, Ultramicroscopy **54**, 31 (1994).

[16]E. Tocha, J. Song, H. Schonherr, and G. J. Vancso, Langmuir **23**, 7078 (2007).

[17]Y. Liu and J. Yang, Nanotechnology **19**, 235501 (2008).

[18]J. Lievonen, K. Ranttila, and M. Ahlskog, Rev. Sci. Instrum. **78**, 043703 (2007).

[19]R. W. Stark, Rev. Sci. Instrum. **75**, 5053 (2004).

[20]C. A. J. Putman, B. G. De Grooth, N. F. Van Hulst, and J. Greve, J. Appl. Phys. **72**, 6 (1992).

[21]E. Hecht, *Optics*, 4th ed. (Addison Wesley Longman, Reading, MA, 2002).

[22]A. Yariv, *Quantum Electronics*, 3rd ed. (Wiley, New York, 1989).

[23]L. O. Heim, M. Kappl, and H. J. Butt, Langmuir **20**, 2760 (2004).

[24]T. Fukuma and S. P. Jarvis, Rev. Sci. Instrum. **77**, 043701 (2006).

[25]D. A. Walters, J. P. Cleveland, N. H. Thomson, P. K. Hansma, M. A. Wendman, G. Gurley, and V. Elings, Rev. Sci. Instrum. **67**, 3583 (1996).

[26]K. Neuman and A. Nagy, Nat. Methods **5**, 491 (2008).

[27]F. Kuhner, J. Morfill, R. A. Neher, K. Blank, and H. E. Gaub, J. Biophysical **92**, 2491 (2007).

[28]V. T. Moy, E. L. Florin, and H. E. Gaub, Colloids Surf., A **93**, 343 (1994).

[29]P. Hinterdorfer and Y. F. Dufrêne, Nat. Methods **3**(5), 347 (2006).

[30]A. Noy, C. D. Frisbie, L. F. Rozsnyai, M. S. Wrighton, and C. M. Lieber, J. Am. Chem. Soc. **117**, 7943 (1995).